Volume 324, number 1, 93–98 FEBS 12555 June 1993

^1H and ^{15}N assignments and secondary structure of the PI3K SH3 domain

Satoshi Koyama[a], Hongtao Yu[a], David C. Dalgarno[b], Tae Bum Shin[a], Lynne D. Zydowsky[b] and Stuart L. Schreiber[a]

[a]*Department of Chemistry, Harvard University, Cambridge, MA 02138, USA* and [b]*ARIAD Pharmaceuticals Inc., Cambridge, MA 02139, USA*

Received 15 April 1993

The sequential ^1H and ^{15}N assignments of the SH3 domain of human phosphatidyl inositol 3′-kinase (PI3K) were determined by a combination of homonuclear and heteronuclear NMR experiments. With the exception of several protons belonging to lysine and proline residues, all proton and proton-bearing amide nitrogen resonances were assigned. Based on the sequential nuclear Overhauser effects (NOEs), $^3J_{NH\text{-}C\alpha H}$ coupling constants and locations of slowly exchanging amide protons, we determined that the secondary structures of the protein consists of six β-strands, two β-turns and four short helices. Additional long range NOEs indicate that these β-strands form two antiparallel β-sheets The topology of secondary structural elements of the PI3K SH3 domain is similar to those of the SH3 domains from c-Src and α-spectrin, suggesting that the SH3 family has a common tertiary structural motif

Nuclear magnetic resonance; Secondary structure; SH3 domain; PI3K

1. INTRODUCTION

The Src homology 2 (SH2) and 3 (SH3) domains are widely distributed among proteins involved in intracellular signaling pathways [1,2]. SH2 domains are known to bind phosphotyrosine-containing peptide sequences; these binding events result in specific localization and states of activation [1]. Although the functions of SH3 domains have not yet been fully clarified, recent studies suggest that certain SH3 domains may link the signaling pathways of tyrosine kinases and guanine nucleotide binding proteins [1,3,4].

The heterodimeric enzyme phosphatidyl inositol-3′-kinase (PI3K) consists of a 110 kDa-subunit that contains the kinase domain and a 85 kDa subunit that contains one SH3 and two SH2 domains [5–7]. This enzyme associates with some receptors or their substrates through one or both of its SH2 domains [5,6,8,9]. The roles of its SH3 domain are less understood. Although the three-dimensional structure of the N-terminal SH2 domain of PI3K was solved [10], no previous structural studies have been carried out on its SH3 domain.

Structural analyses of SH3 domains from the cytoskeletal protein α-spectrin [11] and the signaling protein c-Src [12] have been reported. The three-dimensional structures of the proteins are highly similar, as expected given their significant sequence homology (31%). However, it is difficult to predict the structural features of the SH3 domain of PI3K from these results, because of the lower sequence homology of this domain compared to those of α-spectrin and c-Src and a unique insertion of fifteen amino acid residues found in PI3K [5].

In this paper, we report an analysis of the secondary structure of the SH3 domain of PI3K derived from NMR experiments. This domain consists of the first 85 residues of the protein. To overcome problems due to resonance overlap, the sequential assignment of backbone proton and nitrogen resonances was accomplished using three-dimensional total correlation ^{15}N-^1H heteronuclear multiple quantum coherence spectrum (TOCSY-HMQC) [13] and three-dimensional ^1H nuclear Overhauser enhancement (NOE) ^{15}N-^1H HMQC spectrum (NOESY-HMQC) [13,14]. Patterns of long- and medium-range NOEs have also allowed us to determine the secondary structure of the PI3K SH3 domain. The comparison of its secondary structure with those of c-Src and α-spectrin are also discussed.

Correspondence address S.L. Schreiber, Department of Chemistry, Harvard University, Cambridge, MA 02138, USA.

2. MATERIALS AND METHODS

The SH3 domain of PI3K (MSAEGYQYRALYDYKKEREE-DIDLHLGDILTVNKGSLVALGFSDGQEARPEEIGWLNGY-NETTGERGDFPGTYVEYIGRKKISPP) was overexpressed in *E coli* and purified by column chromatography as described [15]. Uniformly ^{15}N-labeled protein was obtained by growing cells in M9 minimum media containing $^{15}NH_4Cl$ as the sole nitrogen source. The NMR samples were approximately 5 mM protein in a D_2O or 90% H_2O/10% D_2O buffer containing 50 mM potassium phosphate (pH 6.0) and 100 mM KCl. All NMR spectra were recorded at 25°C using either Bruker AMX-600 or AM-500 spectrometers. For the resonance assignment, a series of three- and two-dimensional NMR experiments were carried out: TOCSY-HMQC [13], NOESY-HMQC (τ_m = 150 ms) [13,14], ^1H double quantum filtered-shift correlation spectroscopy

(DQF-COSY), Relay-COSY, double quantum (DQ) spectrum, TOCSY and NOESY (τ_m = 50 and 150 ms). Slowly exchanging amide protons were identified from a 2D ^{15}N-^{1}H HSQC spectrum [16] recorded 3 h after dissolving the lyophilized protein in D_2O buffer. The magnitudes of $^3J_{NH\text{-}C\alpha H}$ coupling constants were obtained qualitatively from an HMQC-J spectrum [17]. All spectra were processed using the program FELIX.

3. RESULTS AND DISCUSSION

3.1. *Identification of spin systems*

PI3K SH3 domain used in this study consists of 85 amino acids: 11 Gly, 4 Ala, 4 Thr, 7 Tyr, 1 His, 2 Phe, 1 Trp, 6 Asp, 3 Asn, 4 Ser, 10 Glu, 2 Gln, 1 Met, 5 Arg, 5 Lys, 4 Pro, 3 Val, 7 Leu, and 5 Ile [5]. The spin systems of all amino acid residues were identified through DQF-COSY, TOCSY, relayed-COSY and DQ spectra measured in both H_2O and D_2O using standard procedures [18,19]. The spin systems of alanine and threonine residues were found in DQF-COSY spectra and confirmed in relayed-COSY spectra. Identification of AMX spin systems, tyrosine, histidine, phenylalanine, tryptophan, aspartic acid, asparagine, and serine, was carried out using TOCSY and relayed-COSY spectra. For the analysis of spin systems of aromatic residues, $C_\beta H$ and ring protons were connected by the strong intra-residue NOEs. Spin systems of glutamic acid, glutamine and methionine were identified by correlation between the amide proton and side chain protons in TOCSY spectra. DQF-COSY and DQ spectra were used to distinguish the $C_\beta H$ and $C_\gamma H$ protons. Arginine spin systems were easily identified through correlations in the amide region of TOCSY spectra, since the pattern of cross-peaks from the backbone NH was the same as that from side chain $N_\varepsilon H$. Since glycine NH/$C_\alpha H$ cross-peaks were usually weak in DQF-COSY spectra, TOCSY and DQ spectra were employed to find this spin system. The spin systems of valine were clarified by correlations from amide protons in TOCSY spectra. Leucine and isoleucine spin systems were identified by the cross-peaks from amide and methyl protons in DQF-COSY, TOCSY and relayed-COSY spectra. Since no cross-peaks for Leu^{26} were observed from amide protons in these spectra, a NOESY spectrum was used to analyze the spin system of this residue. In this study, a DQ spectrum was useful in distinguishing the spin systems of leucine and isoleucine by the remote cross-peaks of C_γ methylene protons in isoleucine. It is difficult to analyze the spin systems of lysine and proline residues due to resonance overlap and limited transfer efficiency along the side chains in TOCSY experiments. Thus, some lysine and proline side chain resonances could not be identified. Though the identification of spin systems was largely obtained from a series of two-dimensional NMR experiments, all assignments were confirmed through three-dimensional TOCSY-HMQC NMR spectra.

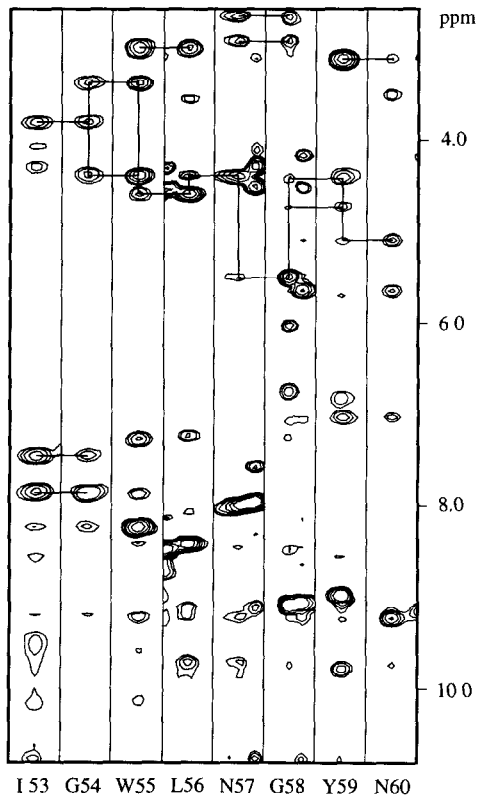

Fig. 1. Three-dimensional NOESY-HMQC strip plots for the region from Ile^{53} to Asn^{60}. Each strip was taken from the 3D spectrum at the ^{15}N chemical shift of an assigned ^{15}N resonance. Continuous solid lines show $d_{\alpha N}$ connectivities through this region. Other straight lines indicate d_{NN} (between Ile^{53} and Gly^{54}) and $d_{\beta N}$ (from Trp^{55} to Asn^{60}) connectivities

3.2. *Sequential assignments*

Sequence specific resonance assignments were obtained by identification of NOEs between adjacent residues in the PI3K SH3 sequence according to standard methods [18,19]. The assignment procedure was performed using both two-dimensional NOESY and three-dimensional NOESY-HMQC experiments. For example, sequential connections from Ile^{53} to Asn^{60} are shown in Fig. 1. The strong sequential $d_{\alpha N}(i,i+1)$ NOEs made it possible to connect residues in the β-strands. Residues in the helices and β-turns could be sequentially connected by $d_{NN}(i,i+1)$ NOEs. Weaker but significant sequential NOEs were observed between residues located in flexible regions [15]. Due to the severe resonance overlap, it was difficult to assign residues in the flexible loop (from Lys^{15} to Glu^{20}) and the C-terminal flexible tail (from Arg^{79} to Pro^{85}). Assignments in these regions relied heavily on the three-dimensional NMR data. In order to make sequential assignments at the positions of the two proline residues, Pro^{50} and Pro^{70}, $d_{\alpha\delta}(i,i+1)$ NOEs were used. Ambiguities resulting from $C_\alpha H$ chemical shift degeneracy or from $C_\alpha H$ overlap with water were solved by the connection through $d_{\beta N}$

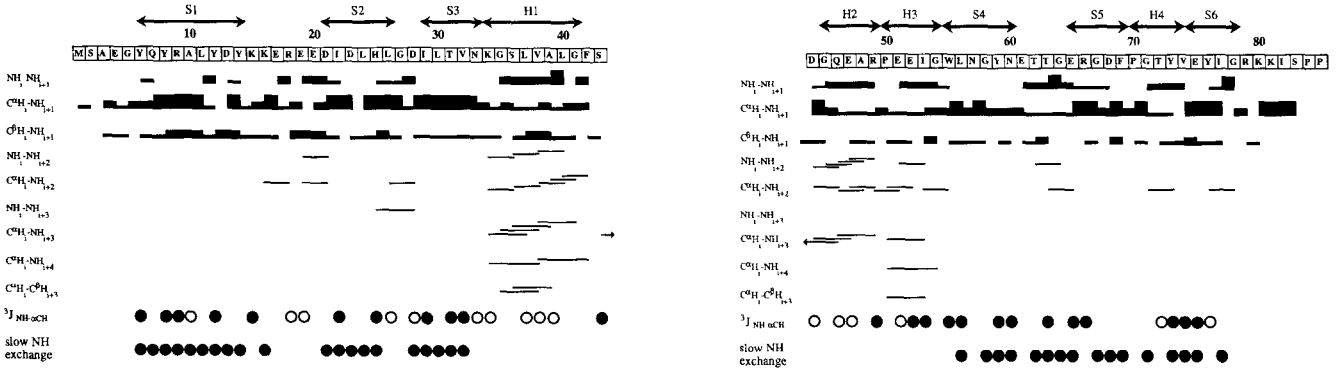

Fig. 2. Summary of sequential NOEs, $^3J_{NH\text{-}\alpha CH}$ coupling constants and slowly exchanging amide protons. The bar heights indicate the intensities of the corresponding NOEs (strong, medium or weak). Medium range NOEs ($2 \leq |i-j| \leq 4$) are shown by straight lines. In the $^3J_{NH\text{-}1C\alpha H}$ row, small coupling constants are shown as open circles, while large coupling constants are shown as closed circles. Slowly exchanging amide protons are represented by closed circles. Above the amino acid sequence, the proposed secondary structural elements are shown; S1–S6 are β-strands and H1–H4 are helices.

NOEs. A summary of the sequential NOEs used to make resonance assignments is demonstrated in Fig. 2. These sequential assignments were confirmed by the compatibility of the spin system identifications. After completion of the sequential connection, some of the uncompleted spin systems were assigned through the intraresidue NOEs in the NOESY spectra. Stereo specific assignments of some $C_\beta H$ methylene protons and some $C_\gamma H_3$ methyl protons of valine were made by analysis of $^3J_{C\alpha H\text{-}C\beta H}$ coupling constants and intraresidue NOEs [20]. In addition, nitrogen resonances were assigned according to amide proton assignments using TOCSY-HMQC and SQC spectra. All assigned ^1H and ^{15}N chemical shifts in the PI3K SH3 domain are listed in Table I.

3.3. *Analysis of secondary structures*

Secondary structural elements were identified by a variety of NMR data including the characteristic NOEs and vicinal coupling constants of backbone protons (Fig. 2). Six β-strands were clarified by strong $d_{\alpha N}(i,i+1)$ NOEs, large $^3J_{NH\text{-}C\alpha H}$ coupling constants and interstrand long range NOEs. These consist of S1(Tyr^6–Tyr^{14}), S2(Asp^{21}–Leu^{26}), S3(Ile^{29}–Asn^{33}), S4(Trp^{55}–Asn^{60}), S5(Glu^{65}–Phe^{69}) and S6(Val^{74}–Gly^{78}). Four helical regions are indicated by strong $d_{NN}(i,i+1)$ NOEs and small $^3J_{NH\text{-}C\alpha H}$ coupling constants together with medium-range NOEs ($2 \leq |i-j| \leq 4$). These consist of H1(Lys^{34}–Gly^{41}), H2(Gly^{45}–Arg^{49}), H3(Pro^{50}–Gly^{54}) and H4(Pro^{70}–Val^{74}). The 38 slowly exchanging amide protons were detected in the SQC spectrum of a freshly prepared sample in D_2O solution. These slowly exchanging protons are likely involved in hydrogen bonds or buried in the hydrophobic core of the protein (Fig. 2). Many of them are located in the deduced β-strands and helices. These data helped to confirm the identification of secondary structural elements described above. Two β-turn structures, T1(His^{25}–Asp^{28}) and T2(Glu^{61}–Gly^{64}), were predicted by strong $d_{NN}(i,i+1)$ and medium $d_{\alpha N}(i,i+2)$ NOEs.

The interstrand long range NOEs and postulated interstrand hydrogen bonds clearly show that two antiparallel β-sheets exist in PI3K-SH3 domain. These are indicated schematically in Fig. 3. One consists of strands S1, S2 and S6, while the other is formed by strands S3, S4 and S5. According to the calculated tertiary structure of this protein, these triple-stranded β-sheets pack against each other at approximately right angles. There is no discontinuity between these two β-sheets, since strands S1 and S3 also form antiparallel β-sheet, as shown in Fig. 3. In addition, parts of strands S2 and S5 are associated with each other in a parallel manner (Fig. 3). A classical β-bulge structure was found in the strand S1, which is indicated by the strong $d_{NN}(i,i+1)$ NOE between Leu^{11} and Tyr^{12}, several interstrand NOEs between strands S1 and S6, and slowly exchanging amide protons of Leu^{11} and Tyr^{12} (Fig. 3). The tertiary structure of the PI3K SH3 domain has been determined using simulated annealing protocols [15]. Fig. 4 shows the three-dimensional fold of this protein, in which the two β-sheets pack against each other thereby enclosing a hydrophobic core.

The topology of the antiparallel β-sheets and the C-terminal helix (H4) of the PI3K SH3 domain are quite similar to those observed in the α-spectrin and c-Src SH3 domains, indicating this topological feature is common among the SH3 family. Structural details, including the β-bulge structure found in strand S1, are also observed in c-Src SH3 domain; however, not in that from α-spectrin. On the other hand, the three short helices found between strands S3 and S4 are unique in the PI3K SH3 domain. According to the sequence alignments of SH3 domains [15], it is interesting that this helix rich region corresponds to the fifteen amino acid insert, which is observed only in the PI3K SH3 domain within the SH3 family.

Table I

^{1}H and ^{15}N chemical shifts[a] of PI3K SH3 domain

Residue	Amide		$C_\alpha H$	$C_\beta H$		Other
	^{15}N	^{1}H		proR	proS	
Met[1]			4.32	1.98, 2.03		$C^\gamma H$ 2.30
Ser[2]	116.3	8.06	4.59	3.82, 3.77		
Ala[3]			4.63	1.53		
Glu[4]	118.0	8.60	4.54	2.07, 1.99		$C^\gamma H$ 2.31, 2.35
Gly[5]	107.1	8.59	4.57, 3.85			
Tyr[6]	119.4	9.45	5.22	3.30, 3.12		$C^\delta H$ 7 31; $C^\varepsilon H$ 6.88
Gln[7]	117.5	9.23	6.10	1.92[d]	1.77[d]	$C^\gamma H$ 2.16, 2.39; $N^\varepsilon H$ 7.41, 7.20; N^ε 110 9
Tyr[8]	117.3	9.46	5.47	2.65[d]	3.02[d]	$C^\delta H$ 7.05, $C^\varepsilon H$ 6.87
Arg[9]	118.2	9.36	5.77	1.93, 1.58		$C^\gamma H$ 1 54; $C^\delta H$ 3.34, 3.25; $N^\varepsilon H$ 7.37; N^ε 81.3
Ala[10]	125.5	9.34	4 74	1.62		
Leu[11]	123.4	9.39	4.10	1.13, 0.81		$C^\gamma H$ 1.52; $C^\delta H$ 0.79, 0.76
Tyr[12]	110 1	7.32	4.84	3.33, 2.62		$C^\delta H$ 6.95; $C^\varepsilon H$ 6.78
Asp[13]	115.3	8.28	4 66	2.78, 2.66		
Tyr[14]	119.5	8 87	4.86	2.98, 2.50		$C^\delta H$ 7.14; $C^\varepsilon H$ 6.90
Lys[15]	127.5	7.78	4.59	1.74, 1.66		$C^\gamma H^b$ 1.46, 1 40; $C^\delta H^b$ 1.55; $C^\varepsilon H$ 3.10
Lys[16]	121.0	8.43	3.89	1.92, 1.84		$C^\gamma H^b$ 1.44, 1.38; $C^\delta H^b$ 1.54; $C^\varepsilon H$ 3.22, 3.02
Glu[17]	120.3	9.28	4.63	2.21, 2.07		$C^\gamma H$ 2.55, 2.38
Arg[18]	118.7	8.77	4.77	1.74, 2.16		$C^\gamma H$ 1.64, 1.57, $C^\delta H$ 3.14, 3.11; $N^\varepsilon H$ 7 33; N^ε 82.5
Glu[19]	118.7	8.75	4.17	2.13, 2.25		$C^\gamma H$ 2.44
Glu[20]	113.0	8.90	4.49	2.02, 1.97		$C^\gamma H$ 2.44, 2.31
Asp[21]	117.7	8.11	5.59	3.24[d]	3 08[d]	
Ile[22]	109.0	8.33	4.79	2.04		$C^{\gamma 2}H$ 0.87; $C^{\gamma 1}H$ 1.12, 0.63; $C^\delta H$ 0.77
Asp[23]	113.6	8.12	4.96	2.53, 2.39		
Leu[24]	114.0	9.28	4.77	2.19, 1.32		$C^\gamma H$ 1.90; $C^\delta H$ 0.90, 0.72
His[25]	119.2	8.27	5.39	3.40[d]	3.26[d]	$C^{\delta 2}H$ 7.50; $C^{\varepsilon 1}H$ 8.63
Leu[26]	122 0	8.66	3.50	1.51[d]	1.73[d]	$C^\gamma H$ 1.55; $C^\delta H$ 0.97, 0.93
Gly[27]	113.7	9.11	4.57, 3.57			
Asp[28]	121.1	8.93	4.77	2.69, 2.73		
Ile[29]	118.2	8.16	5.11	1.91		$C^{\gamma 2}H$ 0.92; $C^{\gamma 1}H$ 1 57, 1.57; $C^\delta H$ 0.83
Leu[30]	123.4	9.48	5.72	1.50, 1.34		$C^\gamma H$ 1.03; $C^\delta H$ 0.46, 0.19
Thr[31]	115.5	9.76	5.51	4.30		$C^\gamma H$ 1.30
Val[32]	128.8	10.15	4.79	2.59		$C^\gamma H$ 1.42, 1.38
Asn[33]	124.4	9.60	4.99	3.14, 3.06		$N^\delta H$ 7.90, 7.20; N^δ 111.0
Lys[34]	124.6	9.14	4.19	1.91, 1.80		$C^\gamma H^b$ 0.90; $C^\delta H^b$ 1.53; $C^\varepsilon H$ 3.12
Gly[35]	102.9	9.10	4.12, 4.02			
Ser[36]	114.7	7.95	4.51	4.28, 4.28		
Leu[37]	119.3	7.55	4.44	2.08, 1.61		$C^\gamma H$ 1.88; $C^\delta H$ 0 91, 0.84
Val[38]	118.1	8.32	3 98	2.24		$C^\gamma HR$ 1.11[d]; $C^\gamma HS$ 1.28[d]
Ala[39]	120.2	8.01	4.24	1.61		
Leu[40]	114.4	7.42	4.42	2.00, 1.75		$C^\gamma H$ 1.99; $C^\delta H$ 1.14, 1.05
Gly[41]	104.3	8.03	4.15, 3.89			
Phe[42]	117.4	7.79	4.88	3.11, 2.97		$C^\delta H$ 7.29; $C^\varepsilon H$ 7.41, $C^\zeta H$ 7.47
Ser[43]	115.1	8.71	4.75	4 03, 3.92		
Asp[44]	120.1	8.72	4.56	2.82, 2.69		
Gly[45]	113 2	9.34	4.44, 3.72			
Gln[46]	117.9	8.28	3.84	1.98, 2.23		$C^\gamma H$ 2.27; $N^\varepsilon H$ 7.57, 7.51; N^ε 111.9
Glu[47]	116.0	9.84	3.63	1.51, 1.44[c]		$C^\gamma H^c$ 1.30, 1.18
Ala[48]	117.7	6.81	3.86	1.30		
Arg[49]	115.9	7.75	5.13	1.79, 1.71		$C^\gamma H$ 1.56, 1 52, $C^\delta H$ 3.38, 3.23; $N^\varepsilon H$ 7.80; N^ε 81.9
Pro[50]			4.07	1.90, 1.79		$C^\gamma H$ 2.40, 1.92, $C^\delta H$ 4.17, 3.56
Glu[51]	117.3	10.13	3 83	2.05, 2 24		$C^\gamma H$ 2.41
Glu[52]	117.3	7.83	4.28	2.09, 2.25		$C^\gamma H$ 2.37
Ile[53]	118.2	7.43	3.79	1.68		$C^{\gamma 2}H$ 0.70; $C^{\gamma 1}H$ 1.33 0.42; $C^\delta H$ 0.51
Gly[54]	106.5	7.84	4.38, 3.37			
Trp[55]	122.3	8.22	4.58	3.01, 2.95		$C^{\delta 1}H$ 7.25; $N^{\varepsilon 1}H$ 10.12; $N^{\varepsilon 1}$ 126 5; $C^{\varepsilon 3}H$ 7 23; $C^{\eta}H$ 7.44; $C^{\zeta 2}H$ 7.54; $C^{\zeta 3}H$ 6.78
Leu[56]	121.5	8.40	4.38	0.21[d]	0.84[d]	$C^\gamma H$ 1.20; $C^\delta H$ 0.67, 0.34
Asn[57]	115.1	7.97	5.49	2.64[d]	2.91[d]	$N^\delta H$ 8.46, 7.07; N^δ 111.3
Gly[58]	109.4	9.07	4.70, 4.40			
Tyr[59]	118.5	8.95	5.11	3.13, 3.07		$C^\delta H$ 7.02; $C^\varepsilon H$ 6.86
Asn[60]	124.1	9.22	4 81	3.50, 2.15		$N^\delta H$ 8.31, 5.70; N^δ 107.5

(continued on page 97)

Table I continued

Residue	Amide		$C_\alpha H$	$C_\beta H$		Other
	^{15}N	^{1}H		proR	proS	
Glu[61]	123.3	9.49	3.95	1.96, 1.90		$C^\gamma H$ 2.54, 2.43
Thr[62]	113.9	8.40	4.14	4.38		$C^\gamma H$ 1.38
Thr[63]	106.9	7.51	4.45	4.47		$C^\gamma H$ 1.28
Gly[64]	110.3	8.84	4.29, 3.92			
Glu[65]	116.3	7.26	4.72	2.03, 1.98		$C^\gamma H$ 2.45, 2.27
Arg[66]	118.1	8.80	5.64	2.05, 1.98		$C^\gamma H$ 1.83, 1.76; $C^\delta H$ 3.44, 3.34; $N^\varepsilon H$ 7.50; N^ε 82.0
Gly[67]	109.5	9.03	4.50, 4.16			
Asp[68]	118.7	8.64	6.02	2.72, 2.72		
Phe[69]	111.5	9.09	5.17	3.15		$C^\delta H$ 6.69; $C^\varepsilon H$ 6.77; $C^\zeta H$ 6.81
Pro[70]			3.56	0.89		$C^\gamma H$ 0.94, 0.38; $C^\delta H$ 2.77, 2.74
Gly[71]	109.8	8.09	3.81, 3.51			
Thr[72]	101.3	7.38	4.15	4.46		$C^\gamma H$ 1.38
Tyr[73]	117.3	7.61	4.88	3.51, 3.03		$C^\delta H$ 7.20; $C^\varepsilon H$ 7.00
Val[74]	106.7	7.42	5.62	2.30		$C^\gamma HR$ 0.86[d]; $C^\gamma HS$ 0.93[d]
Glu[75]	113.6	8.95	5.23	2.24[d]	2.10[d]	$C^\gamma H$ 2.48, 2.35
Tyr[76]	123.3	9 60	4.58	3.06, 3.30		$C^\delta H$ 6.85; $C^\varepsilon H$ 6.76
Ile[77]	120.1	8.49	4.45	1.88		$C^{\gamma 2} H$ 0.85; $C^{\gamma 1} H$ 1.85, 1.09; $C^\delta H$ 0.64
Gly[78]	105.0	5.85	4.38, 3.55			
Arg[79]	115.5	8.44	4.99	1.98, 1.83		$C^\gamma H$ 1.54
Lys[80]	121.3	8.51	4.33	1.75, 1.54		$C^\gamma H^b$ 1.00; $C^\delta H^b$ 1.37; $C^\varepsilon H$ 3.04
Lys[81]	125.0	8.72	4.54	1.87, 1.83		$C^\gamma H^b$ 1.47, 1.37; $C^\delta H^b$ 1.59; $C^\varepsilon H$ 3.08
Ile[82]	120.6	8.46	4.42	1.94		$C^{\gamma 2} H$ 1.00; $C^{\gamma 1} H$ 1.51, 1.20; $C^\delta H$ 0.91
Ser[83]	119.9	8.61	4.92	3.98, 3.85		
Pro[84]						
Pro[85]						

[a]Chemical shifts are reported for the PI3K SH3 domain at pH 6.0 and 298K in 50 mM potassium phosphate buffer containing 100 mM KCl. Proton chemical shifts are referenced to H_2O at 4.86 ppm. Nitrogen chemical shifts are referenced to external $^{15}NH_4Cl$ (5 M) in 1 M aqueous HCl at 26.1 ppm.
[b]Unable to distinguish between $C^\gamma H$ and $C^\delta H$.
[c]Unable to distinguish between $C^\beta H$ and $C^\gamma H$.
[d]Stereospecifically assigned.

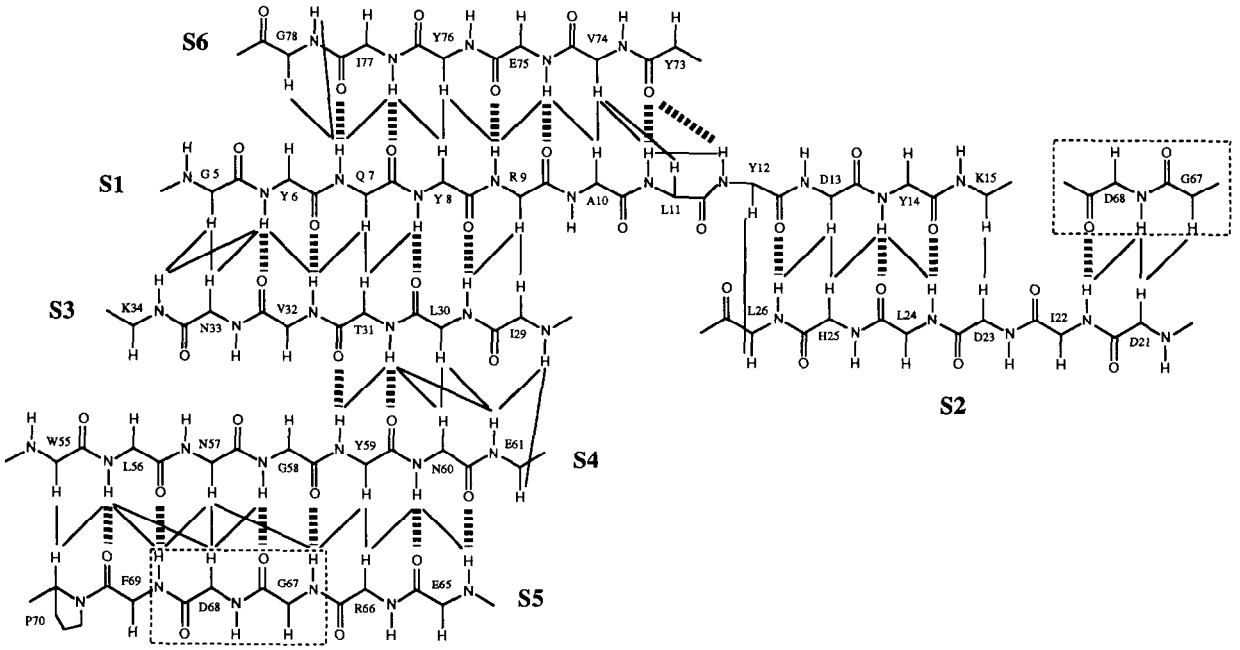

Fig. 3. A schematic diagram of the inter-strand NOEs in the β-sheet regions of the PI3K SH3 domain. Solid lines indicate inter-strand NOEs and dashed lines show deduced hydrogen bonds from slowly exchanging amide protons and long-range NOEs. The region from Gly[67] to Asp[68] in strand S5, which is enclosed by a dashed square, forms an antiparallel β-sheet with the strand S4 and associates with the strand S2 in parallel manner.

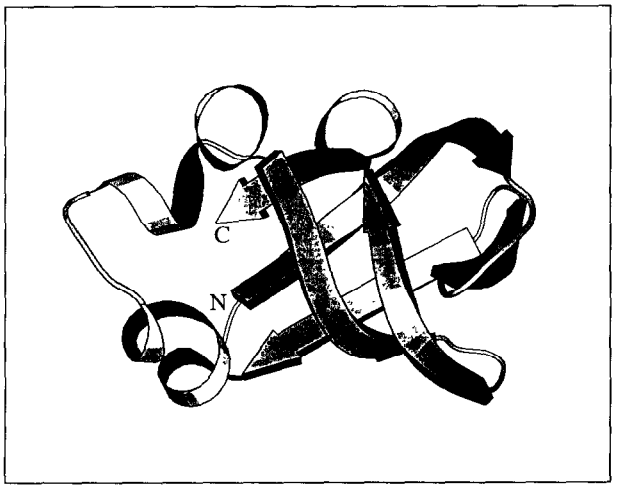

Fig. 4. Three-dimensional structure of the PI3K SH3 domain calculated by simulated annealing protocols. N- and C-terminals are labeled by N and C, respectively. This diagram was drawn using the program MOLSCRIPT [21].

In conclusion, the resonance assignments for the PI3K SH3 domain have been determined and the secondary structure of the protein has been analyzed. The results indicate that SH3 domains may have a common topological feature of the secondary structural elements. This information, as well as the three-dimensional structure of the PI3K SH3 domain, will aid in understanding the functions of this domain.

Acknowledgements: We thank M.K. Rosen (Harvard University) for assistance with the sequential assignments and C. Anklin (Bruker Instruments) for a generous gift of instrument time. This research was supported by a grant from the National Institute of General Medical Sciences (GM-44993), a sabbatical fellowship from Fujisawa Pharmaceutical Co., Ltd. (to S.K.) and a predoctoral fellowship from the Natural Sciences and Engineering Research Council of Canada (to T.B.S.).

REFERENCES

[1] Pawson, T. and Gish, G.D. (1992) Cell 71, 359–362.
[2] Musacchio, A., Gibson, T., Lehto, V.P. and Saraste, M. (1992) FEBS Lett. 307, 55–61.
[3] Williams, L.T. (1992) Curr. Biol. 2, 601–603.
[4] Lowenstein, E.J., Daly, R.J., Datzer, A.G., Li, W., Margolis, B., Lammers, R., Ullrich, A.L., Skolnik, F.Y., Bar-Sag, H. and Schlessinger, J. (1992) Cell 70, 431–442.
[5] Skolnik, E.Y., Margolis, B., Mohammadi, M., Lowenstein, E., Fischer, R., Drepps, A., Ullrich, A and Schlessinger, J. (1991) Cell 65, 83–90
[6] Otsu, M., Hiles, I., Gout, I., Fry, M.J., Ruiz-Larrea, F., Panayotou, G., Thompson, A., Dhand, R., Hsuan, J., Totty, N., Smith, A.D., Morgan, S.J., Courtneidge, S.A., Parker, P.J. and Waterfield, M.D. (1991) Cell 65, 91–104.
[7] Hiles, I.D., Otsu, M., Volinia, S., Fry, M.J., Gout, I., Dhand, R., Panayotou, G., Ruiz-Larrea, F., Thompson, A., Totty, N.F., Hsuan, J.J., Courtneidge, S.A., Parker, P.J. and Waterfield, M.D. (1992) Cell 70, 419–429.
[8] Varticovski, L., Druker, B., Morrison, D., Cantley, L.C. and Roberts, T.M. (1989) Nature 342, 699–702.
[9] Sun, X.J., Rothenberg, P., Kahn, C.R., Backer, J.M., Araki, E., Wilden, P.A., Cahill, D.A., Goldstein, B.J. and White, M.F. (1991) Nature 352, 73–77.
[10] Booker, G.W., Breeze, A.L., Downing, A.K., Panayotou, G., Gout, I., Waterfield, M.D. and Campbell, I.D. (1992) Nature 358, 684–687.
[11] Musacchio, A., Noble, M., Pauptit, R., Wierenga, R. and Saraste, M. (1992) Nature 359, 851–855.
[12] Yu, H., Rosen, M.K., Shin, T.B., Seidel-Dugan, C., Brugge, J.S. and Schreiber, S L. (1992) Science 258, 1665–1668.
[13] Marion, D., Driscoll, P.C., Kay, L.E., Wingfield, P.T., Bax, A., Gronenborn, A.M. and Clore, G.M (1989) Biochemistry 28, 6150–6156.
[14] Zuiderweg, E.R.P. and Fesik, S W. (1989) Biochemistry 28, 2387–2391.
[15] Koyama, S., Yu, H., Dalgarno, D.C., Shin, T.B., Zydowsky, L.D. and Schreiber, S.L. (1993) Cell 72, 945–952.
[16] Bax, A., Griffey, R.H. and Hawkins, B L. (1983) J. Am Chem. Soc. 105, 7188–7190.
[17] Kay, L.E and Bax, A. (1990) J. Magn. Reson. 86, 110–126.
[18] Chazin, W.J., Rance, M and Wright, P E. (1988) J. Mol. Biol. 202, 603–622.
[19] Chazin, W.J. and Wright, P.E. (1988) J. Mol. Biol. 202, 623–636.
[20] Wagner, G., Braun, W., Havel, T.F., Schaumann, T., Go, N. and Wuthrich, K. (1987) J. Mol. Biol. 196, 611–639.
[21] Kraulis, P.J. (1991) J. Appl Crystallogr. 24, 946–950.